Original Article

PARAGONIMUS HETEROTREMUS INFECTION IN NAGALAND: A NEW FOCUS OF PARAGONIMIASIS IN INDIA

*TS Singh, H Sugiyama, A Umehara, S Hiese, K Khalo

Abstract

Purpose: To determine the prevalence of paragonimiasis among the patients who were attending the tuberculosis (TB) clinics at the Community Health Centre, Pfutsero, Phek District, Nagaland. To determine the species of *Paragonimus* that cause infection in humans and the crustacean host that acts as the infectious source for humans. **Materials and Methods:** Sputum specimens were examined microscopically for Paragonimus eggs and acid fast bacilli. Blood samples were tested by microenzyme-linked immunosorbant assay for Paragonimus-specific immunoglobulin G antibodies. Crab extracts prepared by digestion with artificial gastric juice were examined for *Paragonimus metacercariae* under a stereoscopic microscope. The species identification of the parasite was based on morphological and molecular characterizations of eggs and metacercariae employing polymerase chain reaction and DNA sequencing. **Results:** Seven out of the 14 patients tested seropositive for paragonimiasis and Paragonimus eggs were detected in sputum of two out of the seven seropositive patients, indicating a prevalence of 50% and an egg detection rate of 14%, respectively. The prevalence was highest in the 10-30 year age group. More males got the infection than females, the ratio being 5:2. *P. heterotremus* was identified as the causative agent of human paragonimiasis and *Potamiscus manipurensis* as the crab host. **Conclusions:** The study revealed that paragonimiasis has been endemic in Pfutsero, Nagaland, and half of the patients attending the TB clinic were actually suffering from pulmonary paragonimiasis. This is the first confirmed report of an endemic focus of paragonimasis and description of *P. heterotremus* as the causative agent in Nagaland, India.

Key words: *India, lung fluke, Nagaland, paragonimiasis, P. heterotremus, tuberculosis*

Introduction

Lung flukes have been described in the world, mainly from East and Southeast Asia and also from Africa and Americas. *Paragonimus westermani*, the most widely distributed species in Asia, was first described by Kerbert from the lungs of a Bengal tiger, which was captured in India and died at a zoo in Amsterdam more than a century ago. However, very little attention has been paid to this parasite because paragonimiasis was never considered to be a public health problem in India and had remained a neglected disease until the first case was reported from Manipur in 1982.[1] After that, many cases were reported from several parts of Manipur.[2-4] Subsequently, endemic foci of paragonimiasis were also discovered in Arunachal Pradesh.[5] Most interestingly, *P. heterotremus* has been identified as the causative agent of human paragonimiasis in this part of India against the widely believed *P. westermani*, which was reported from many mammals in India.

In the past, some occasional cases from Nagaland, initially diagnosed as pulmonary TB by clinical symptoms and chest X-rays, were referred to the Regional Institute of Medical Sciences, Imphal, Manipur. The cases were parasitologically confirmed as pulmonary paragonimiasis. However, detailed information on the prevalence of paragonimiasis in the northeast states of India other than Manipur and Arunachal Pradesh were limited. The present study was, therefore, performed to ascertain the prevalence of paragonimiasis among the patients who were attending the TB clinic at the Community Health Centre, Pfutsero, Nagaland, and to determine the causative species and some of the epidemiological factors responsible for the infection.

Materials and Methods

Patients and clinical examination

The senior author visited the Community Health Centre at Pfutsero town, Phek district, Nagaland, during March 27-28, 2008 to investigate paragonimiasis among the patients attending the TB clinic at the health centre. Pfutsero town is located in southeast Nagaland, bordering Manipur in the south and Myanmar in the east.

Detailed clinical history taking and physical examination of all the patients were performed by the medical officers. The findings were recorded in a pre-designed profoma printed in English. Informed consent about the examination and procedures was obtained from each patient after proper explanation in their own dialect. Postero-anterior chest

*Corresponding author (email: <shantikumar_singh@rediffmail. com>) Department of Microbiology (TSS), Sikkim Manipal Institute of Medical Sciences, 5th mile, Tadong - 737 102, Gangtok, Sikkim, India, Department of Parasitology (HS,AU), National Institute of Infectious Diseases, Tokyo, Japan. Community Health Centre (SH,KK), Pfutsero, Phek, Nagaland, India

roentgenograms were taken for all the patients to evaluate any abnormal lesion in the chest.

Sputum examination

The sputum samples of the patients were collected in sterile plastic screw-capped containers. The specimens were examined microscopically for Paragonimus eggs and also for acid fast bacilli (AFB) using the wet cover slip smears and Ziehl-Neelsen-stained smears, respectively. The Paragonimus eggs were then preserved in two parts, one portion in equal volume of 10% phosphate-buffered formalin for morphological study and another in equal volume of 70% ethanol for molecular characterization.

Microenzyme-linked immunosorbant assay (ELISA) test

The blood samples of all the patients were tested for Paragonimus immunoglobulin G antibodies by micro-ELISA using antigens prepared from adult *P. heterotremus* worms.[6] Optical density (OD) values higher than 0.300 were taken as positive.

Examination of crabs

A total of 20 fresh water crabs were collected from a "Zachughie" mountain stream near the Pfutsero town. After morphological examination, the crabs were extracted and then digested with artificial gastric juice, followed by differential filtration.[7] The filtrates were examined under a stereoscopic microscope for *P. metacercariae*. The isolated metacercariae were preserved in two separate vials containing 10% formol-saline and 70% ethanol for morphological and molecular characterization, respectively.

Morphological and molecular characterization

Morphological features of eggs from the patients and metacercariae from the crabs were examined microscopically. Molecular characterization of eggs and metacercariae was performed by DNA isolation, amplification of the ITS2 regions of the ribosomal DNA by polymerase chain reaction (PCR)-linked restriction length polymorphism method and sequencing.[8,7] To be more precise, the primers used were 3S (forward, 5'-GGTACCGGTGGATCACTCGGCTCGTG-3')[9] and A28 (reverse,5'-GGGATCCTGGTTAGTTTCTTTTCCTCCGC-3'). [10] The PCR amplification was performed using 0.25 μm of each primer and 2.5 U of Taq polymerase (Invitrogen Corp., Carlsbad, CA, USA). The amplified products were extracted from agarose gels (Lonza, Rockland, ME, USA) and sequenced using the corresponding primers and the BigDye Terminator Cycle Sequencing kit (Applied Biosystems, Foster City, CA, USA) on an automated sequencer (ABI 310 Genetic Analyzer; Applied Biosystems). The amplified products (10 μm) were also treated with 5 U of the restriction enzyme *Apa*LI (New England Biolabs, Beverly, MA,

USA) at 37°C for 1 h. The amplicons with or without the enzymatic treatment were then separated by electrophoresis on 2% (w/v) agarose gels.

Results

A total of 14 patients who attended the TB centre with some respiratory symptoms were investigated. The major clinical manifestations presented by them are shown in Table 1. Chronic productive cough was the most common of all the complaints followed by difficulty in breathing and recurrent haemoptysis. In three patients, the sputum smears showed AFB while Paragonimus eggs were all negative. In 11 patients who were negative for AFB, two patients discharged Paragonimus eggs in the sputum. These two patients and four other patients who were negative for Paragonimus egg and AFB were positive for antibodies against the Paragonimus antigen. One smear-positive TB patient was also seropositive against the Paragonimus antigen. In summary, seven out of the 14 patients were positive for antibodies against the Paragonimus antigen. The OD values of the seropositive cases varied from 0.34 to 1.53, with 0.82 on average. Two patients who were egg positive showed much higher OD values (1.53 and 1.36) than the egg negative but seropositive patients.

Of the seven paragonimiasis cases, there were five male and two female, making a male-to-female ratio of 5:2. In addition, a higher prevalence of paragonimiasis was detected among children and young adults in the age group of between 7 and 32 years and rare after 40 years of age. The chest roentgenograms showed abnormal areas in three of the seven seropositive patients (paragonimiasis). Left-sided pleural effusions were seen in two patients whose sputa were Paragonimus egg positive and right lung pneumonia in another seropositive patient. Out of the three TB patients, no abnormal lesions were detected in two while nodular shadows were seen in the right upper lung in one. This patient was infected with both Paragonimus (seropositive) and TB. Fever, weakness, weight loss and loss of appetite were found as other associated symptoms in this patient.

Table 1: Major clinical manifestations and laboratory examination findings observed in 14 patients	
Clinical manifestations and laboratory findings	No. of patients (%)
Cough	14 (100)
Difficult breathing	9 (64)
Recurrent haemoptysis	6 (43)
Fever	6 (43)
Pain in the chest	3 (21)
Acid fast bacilli (AFB)	3 (21)
Anti-Paragonimus antibodies (Ab)	7 (50)
Paragonimus eggs	2 (14)
Both AFB and Ab	1 (7)

The morphological features of the eggs from the two patients [Figure 1a] were found to be characteristic of *P. heterotremus* with some variations in the shape and size. They were oval and elongated in shape, golden-yellow in colour and operculated and measured 82-95 μm (average = 82 μm) in length and 45-58 μm (average = 49 μm) in width. The eggshell thickness was almost uniform and indiscernible at the non-operculated end.

The freshwater crabs captured in the stream near Pfutsero town were morphologically identified as *Potamiscus manipurensis* [Figure 1b]. Of the 20 freshwater crabs examined, 48 *P. metacercariae* were isolated. Five smaller crabs (carapace size: 20.5 mm × 24.5 mm on average) and 15 larger crabs (carapace size: 29 mm × 37 mm on average) yielded 30 and 18 metacercariae, respectively. The number of metacercariae per crab was higher in smaller crabs (average = 6) than in bigger crabs (average = 1.2). The fresh metacercariae [Figure 1c] were oval to suboval in shape, with a thin outer cyst wall and a thicker inner cyst wall, which was typically thickened at both poles, better defined in Figure 1d. The inner cyst measured on average 197 μm in the long

axis and 163 μm in the transverse axis. The thickness of the inner wall was on average 6.4 μm on the side and gradually thickened at the pole to 18.5 μm on average. The oral sucker was smaller than the ventral sucker and was provided with a stylet. The morphological features of the metacercariae were characteristic of *P. heterotremus*.

By PCR amplification, the ITS2 PCR products of about 520 bp were generated from the DNA samples prepared from the eggs from patients [Figure 2, lane 1] and metacercariae. Two fragments (about 350 bp and 170 bp, Figure 2. lane 2) were generated from the PCR products (520 bp) after digestion with a restriction enzyme *Apa*LI, which recognizes the sequences from *P. heterotremus*.[11] The PCR products were excised from agarose gels after electrophoresis and were used for sequence analysis. The analysis revealed that the aligned ITS2 regions were 461 bp (without primer sequences) for both eggs and metacercariae. The obtained sequence data were deposited in the database GenBank/EMBL/DDBJ under accession numbers AB456558 and AB456559 for the metacercariae and eggs, respectively. They were the identical sequences. Similarity searches of
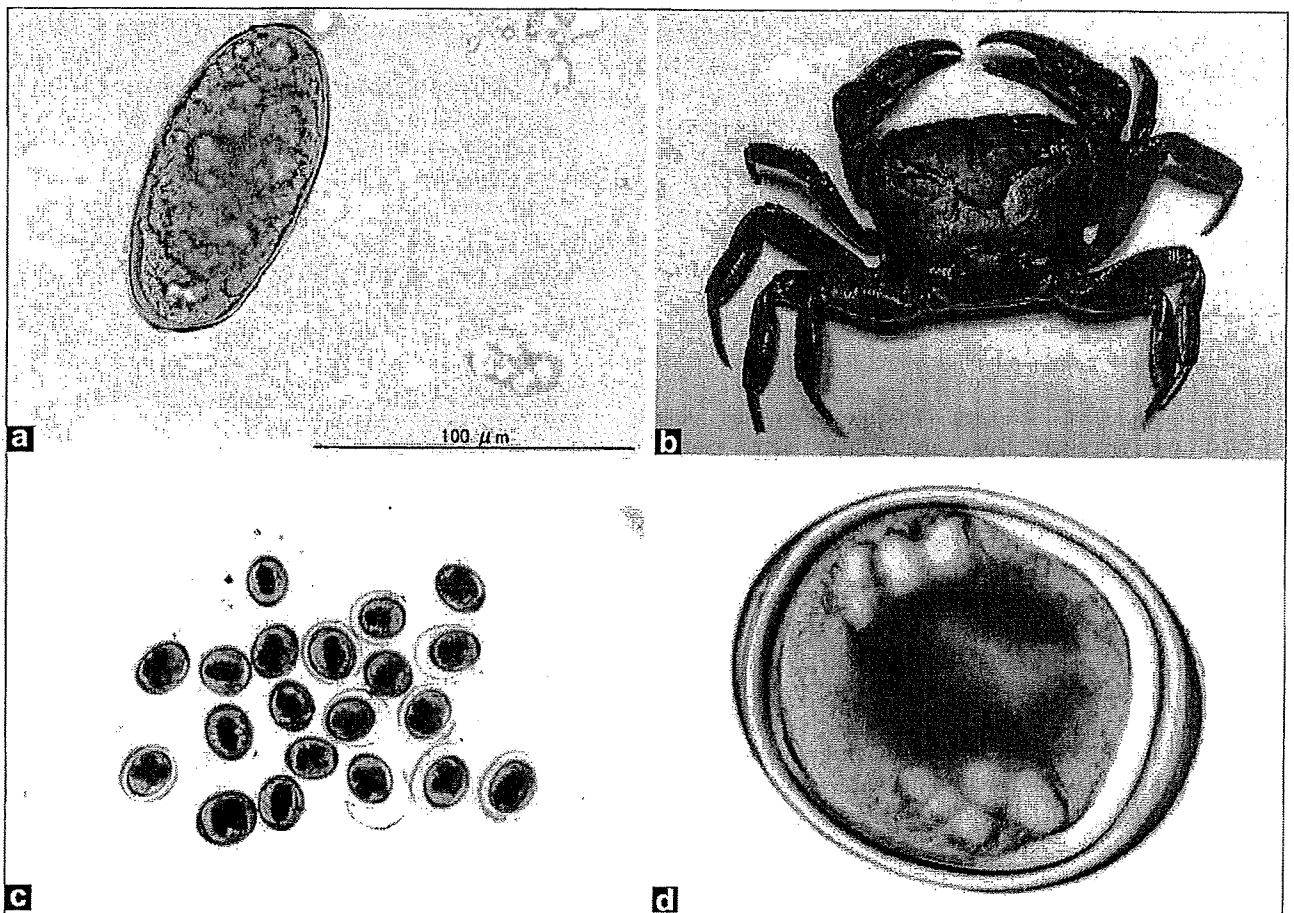

Figure 1: (a) Photomicrographs of formalin (10%)-preserved Paragonimus eggs (×40) found in the sputum examination. (b) Photograph of *Potamiscus manipurensis*, the crab host of *Paragonimus heterotremus*, collected from a mountain stream in Pfutsero town, Nagaland. (c) *P. heterotremus* metcarcariae (×10) isolated from *Potamiscus manipurensis*. (d) Single metacercariae (×40). Note the oval-shaped and thickened cyst wall at either pole
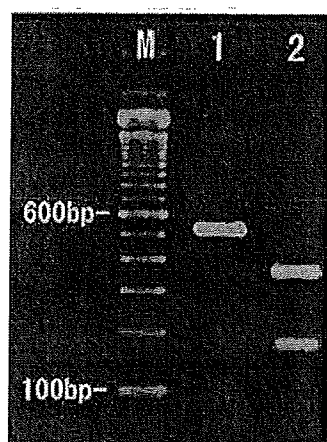
Figure 2: Results of polymerase chain reaction (PCR) (lane 1, a band of about 520 bp) and PCR-restriction fragment length polymorphism with *ApaLI* (lane 2, two fragments of about 350 bp and 170 bp) using the DNA sample isolated from the eggs from one patient. The same results were obtained when we used DNA samples isolated from the eggs of another patient or those from the metacercariae. Hundred basepair DNA ladders (Invitogen) were used to estimate the sizes of the bands (lane M)

the database revealed that the obtained sequences were identical to those from the metacercariae (AB308377) and eggs (AB308378) of *P. heterotremus* occurring in Manipur, India.[7]

Discussion

Although some occasional cases of paragonimiasis, which diagnosed initially as pulmonary TB, were already discovered in Nagaland, the detailed information about the disease was not available. The senior author, therefore, visited the health centre at Pfutsero in Nagaland to investigate further for paragonimiasis and Paragonimus during March 28-29, 2008. We determined the prevalence of paragonimiasis, and the egg detection rate of 14 patients who attended the health centre was 50% and 14%, respectively. The results of morphological and molecular characterization of Paragonimus eggs from sputum samples have established that *P. heterotremus* was the causative agent of paragonimiasis in Nagaland. This species has also been identified as a significant cause of human pulmonary paragonimiasis in Manipur and Arunachal Pradesh, India,[1-5] as well as in Southeast Asian countries like Thailand, Lao PDR and Vietnam.[12]

We also determined the epidemiological factors responsible for infections with *P. heterotremus*. A high prevalence rate of 64% was observed in children and young adults (age ≤ 30). This finding was in agreement with that in Manipur in which two-thirds of the patients were in the age group of 11-30 years[2] and in Arunachal Pradesh in which the infection was higher (52%) in children (age ≤ 15).[13] Crabs are abundant in most of the mountain streams in the endemic areas in Nagaland. The villagers believed that raw crabs or its extract and soup provided them strength and nutrition. Some

believed that ingestion of raw crab extract can cure fever and allergy. These activities are important modes of infection for local people, especially for the young adults. Therefore, it is imperative to undertake health educational programs for the prevention of paragonimiasis in this endemic area.

General physical conditions of paragonimiasis were relatively good. The patients were quite ambulatory and apparently healthy looking. The symptoms were exacerbated just by hard physical activities, which often initiated bouts of haemoptysis. Generally, clinical symptoms and radiological appearances of paragonimiasis were overlapping with pulmonary TB thus resulting in an overdiagnosis of the non-tubercular cases as smear-negative pulmonary TB. Therefore, a detailed clinical history of illness, including dietary habit of consumption of crabs and laboratory investigation such as sputum examinations for Paragonimus eggs and serodiagnoisis, are essentially important in all cases with respiratory symptoms to avoid misdiagnosis. Once diagnosed as paragonimiasis, the disease can be effectively treated with praziquantel.

Conclusion

The result of this investigation revealed the first recognized endemic area of paragonimiasis in Nagaland. Fifty per cent of the patients who were attending the TB clinic with some respiratory symptoms were found to be suffering from pulmonary paragonimiasis based on a serological micro-ELISA test. Two patients who presented with bloody sputum showed Paragonimus eggs in the sputum smears. The infection was common in children and young adults up to 30 years. The chest roentgenograms were normal except in four of the seven seropositive patients. The clinical and radiological features of pulmonary paragonimiasis and TB are similar and, therefore, it should be emphasized that serodiagnosis and sputum examination for Paragonimus eggs are essential before concluding a case as smear-negative pulmonary TB.

References

1. Singh YI, Singh NB, Devi SS, Singh YM, Razaque M. Pulmonary paragonimiasis in Manipur. Indian J Chest Dis Allied Sci 1982;24:304-6.
2. Singh TS, Mutum SS, Razaque MA. Pulmonary paragonimiasis: Clinical features, diagnosis and treatment of 39 cases in Manipur. Trans R Soc Trop Med Hyg 1986;80:967-71.
3. Singh TS, Singh PI, Singh LB. Paragonimiasis: Review of 45 cases. Indian J Med Microbiol 1992;10:243-7.
4. Singh TS, Mutum S, Razaque MA, Singh YI, Singh EY. Paragonimiasis in Manipur. Indian J Med Res (A) 1993;97: 247-52.
5. Narain K, Devi RK, Mahanta J. Paragonimus and paragonimiasis: A new focus in Arunachal Pradesh, India. Curr Sci 2003;84:985-7.
6. Sugiyama H, Sugimoto M, Akasaka K, Horiuchi T, Tomimura T, Kozaki S. Characterization and localization of *Paragonimus westermani* antigen stimulating antibody formation in both the

infected cat and rat. J Parasitol 1987;73:363-7.

7. Singh TS, Sugiyama H, Rangsiruji A, Devi KR. Morphological and molecular characterizations of *Paragonimus heterotremus*, the causative agent of human paragonimiasis in India. Southeast Asian J Trop Med Pub Health 2007;38:82-6.

8. Sugiyama H, Morishima Y, Kameoka Y, Kawanaka M. Polymarase chain reaction (PCR)-based molecular discrimination between *Paragonimus westermani* and *P. miyazaki* at the metacercarial stage. Mol Cell Probes 2002;16:231-6.

9. Bowles J, Blair D, McManus DP. A molecular phylogeny of the human Schistosomes. Mol Phylog Evol 1995;4:103-9.

10. Blair D, Agatsuma T, Watanobe T, Okamaoto M, Ito A. Geographical genetic structure within the human lung fluke, *Paragonimus westermani*, detected from DNA sequences. Parasitology 1997;115:411-7.

11. Sugiyama H, Morishima Y, Rangsiruji A, Binchai S, Ketusat P,

Kameoka Y, *et al.* Molecular discrimination between individual metacercariae of *Paragonimus heterotremus* and *P. westermani* occurring in Thailand. Southeast Asian J Trop Med Public Health 2005;36:102-6.

12. Blair D, Xu ZB, Agatsuma T. Paragonimiasis and the genus Paragonimus. Adv Parasitol 1999;42:113-222.

13. Devi KR, Narain K, Bhattacharya S, Negmu K, Agatsuma T, Blair D, *et al.* Pleuropulmonary paragonimiasis due to *Paragonimus heterotremus*: Molecular diagnosis, prevalence of infection and clinicoradilogical features in an endemic area of northeastern India. Trans R Soc Trop Med Hyg 2007;101: 786-92.

Records of Three Species of Freshwater Crabs from China

TAKEDA Masatsune, SUGIYAMA Hiromu and QIAN Bao-Zhen

Records of Three Species of Freshwater Crabs from China

TAKEDA Masatsune[1], SUGIYAMA Hiromu[2] and QIAN Bao-Zhen[3]

中国産サワガニ類3種の記録

武田　正倫[1]・杉山　広[2]・銭　宝珍[3]

摘　要

中国産のサワガニ類3種，すなわち浙江省産の*Sinopotamon chekiangense* Tai & Song, 1975, 湖北省産の *S. teritisum* Dai, Chen, Zhang & Lin, 1986 および广西自治区産の *Potamon flexum* Dai, Song, Li & Liang, 1980について，写真を付して再記載を行った。

Abstract

Three species of freshwater crabs (Family Potamidae) from China, *Sinopotamon chekiangense* Tai & Song, 1975 from Zhejiang Province, *S. teritisum* Dai, Chen, Zhang & Lin, 1986 from Hubei Province, and *Potamon flexum* Dai, Song, Li & Liang,1980 from Guangxi Zhuang Autonomous Region, are recorded. Each species is described, with some photographs of the distinguishing characters for further identification.

Keywords : Freshwater crab, *Sinopotamon chekiangense*, *Sinopotamon teritisum*, *Potamon flexum*, Hubei Province, Zhejiang Province, Guangxi Zhuang Autonomous Region, China

Introduction

In 2006 and 2007, under the financial supports from the Ministry of Health, Labor and Welfare of Japan on emerging and reemerging diseases and from the Overseas Research Entrustment Program of the Japan Health Sciences Foundation on emerging and reemerging diseases, the junior authors visited several places in China to collect the freshwater crabs as the second intermediate host of the lung flukes. Most of the crabs collected were exposed to the detection of larval cysts of the parasites, and a pair of each species was transmitted to the senior author to know the scientific names of the crabs as a part of a serial study on the Chinese lung flukes.

1) Corresponding author. Faculty of Modern Life, Teikyo Heisei University, 2-51-4 Higashi-Ikebukuro,
   Toshima-ku, Tokyo, 170-8445 Japan; e-mail takeda-m@thu.ac.jp
   東京都豊島区東池袋2-51-4　帝京平成大学　現代ライフ学部
2) Department of Parasitology, National Institute of Infectious Diseases, Tokyo, Japan
   国立感染症研究所　寄生動物部
3) Institute of Bio-engineering, Zhejiang Academy of Medical Sciences, Zhejiang, China
   中国浙江省医学科学院　生物工程研究所

The chelipeds are very slightly different in size and not much inflated. The armature and hairiness of the chelipeds and ambulatory legs are also weaker than in the male. The abdomen is subovate and covers the whole sternum; the sixth and terminal segments are subequal in length, with the terminal segment is subtruncated at the distal margin. The genital orifice is elliptical, one third as wide as the sternum, occupying the anterior half or more at inner part of the sternum.

Remarks. This species has been known by the original paper (Tai & Sung, 1975[2]) and Dai (1991[3], 1999[1]). The male first pleopod is somewhat different from the schematic figures given by the original authors in having the distal segment not so strongly tapering. The general shape of the carapace is typical for *Sinopotamon*, but the carapace is more or less quadrate, with the weakly convergent posterolateral margins of the carapace. The distal segment of the male abdomen is prominent, not tapering, with rounded terminal margin.

Distribution. Known from many localities in Zhejiang Province and some localities in Fujian Province, living under stone in mountain stream.

Notes. Metacercariae of *Paragonimus westermani* (Kerbert, 1878) were isolated.

Sinopotamon teritisum Dai, Chen, Zhang & Lin, 1986
(Figs. 1B, 2B, 4)

Material examined. Guanshan Town, Danjiangkou City, Hubei Province, China （湖北省牡丹口市官山鎮） － 1♂ (cb 31.6 mm, cl 24.6 mm), 1♀ (cb 25.0 mm, cl 19.7 mm), Sept. 7, 2006.

Description. Male. Carapace rather narrow, and ratio of carapace length to breadth 1.2 (Fig. 1B), not convex dorsally (Fig. 2B); dorsal surface divided into regions with shallow depressions, uniformly and rather densely covered with microscopic pits and short hairs; frontorbital margin thin, with supraorbital margin raised dorsally; a transverse depression behind frontorbital margin followed by obtuse anterior ridges of epigastric, protogastric and branchial regions; anterior part of a longitudinal bifurcation separating gastric regions of both sides distinct and linear, but its posterior half obsolete; lateral margins of mesogastric region linear, deep and longitudinal; cardiac region not convex, as large as mesogastric region; metagastric region outside of cardiac region rounded, surrounded by a shallow depression. Anterolateral margin of carapace with a small interruption at hepatic part, being fringed with a series of sharp granules; external orbital angle sharp, directed forward; posterolateral margin of carapace more or less concave.

Chelipeds of both sides slightly unequal, roughened with sharp granules and short hairs. Ambulatory legs strongly depressed, provided with longish hairs mainly on anterior margins; each carpus with a longitudinal, narrow furrow on middle part of upper surface, each propodus with a longitudinal, wide depression occupying two thirds of upper surface.

Abdomen moderately wide, long; sixth segment 1.5 times as long as fifth segment, 2.3 times as wide as long; terminal segment as long as sixth segment, tongue-shaped, tapering distally, with subacute distal margin, being abruptly widened close to articulation with sixth segment. Male first pleopod stout, with distal segment about one third as long as shaft, directed sternally along sternal trench; ventral surface of distal part of shaft more or less callous and thickened; terminal segment weakly directed outward, tapering distally; semitransparent tip one fourth as long as distal segment, narrowing abruptly toward genital orifice at its top.

Female. The general shape and areolation of the carapace are very close to those of the male examined; the dorsal surface is divided into the regions by depressions, and covered with microscopic pits and short hairs; the epigastric areolae behind the frontal margin is more prominent and advanced than in the male. Both
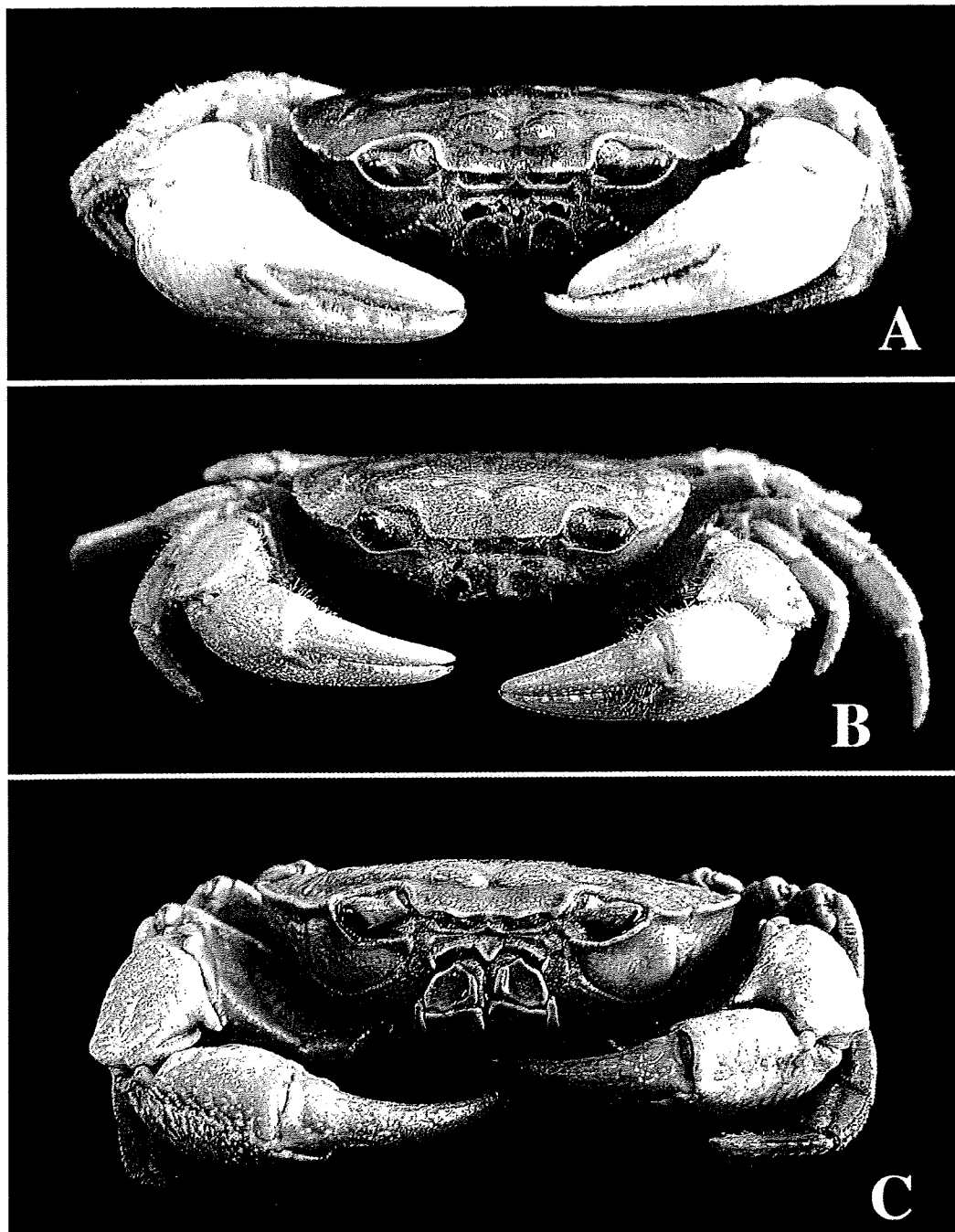
Fig. 2. A: *Sinopotamon chekiangense* Tai & Song, male (cb 35.3 mm) from Yuyao, Zhejiang Province. B: *Sinopotamon teritisum* Dai, Chen, Zhang & Lin, male (cb 31.6 mm) from Danjiangkou, Hubei Province. C: *Potamon flexum* Dai, Song, Li & Liang, male (cb 56.3 mm) from Baiswe, Guangxi Zhuang Autonomous Region.

chelipeds are different in size, but smaller than those of the male. The abdomen is typically ovate and weakly convex along the lateral margins, with the prominent sixth and terminal segments; the sixth segment is one third as long as wide, and the terminal segment is as long as the sixth segment, rather strongly convex forward along the distal margin. The genital orifices are large, occupying almost half, or more, of the sixth sternal segment.

Remarks. This species is generally close to the preceding species, *Sinopotamon chekiangense* Tai & Song, but the carapace is covered with microscopic pits and short hairs, and narrower posteriorly with more strongly
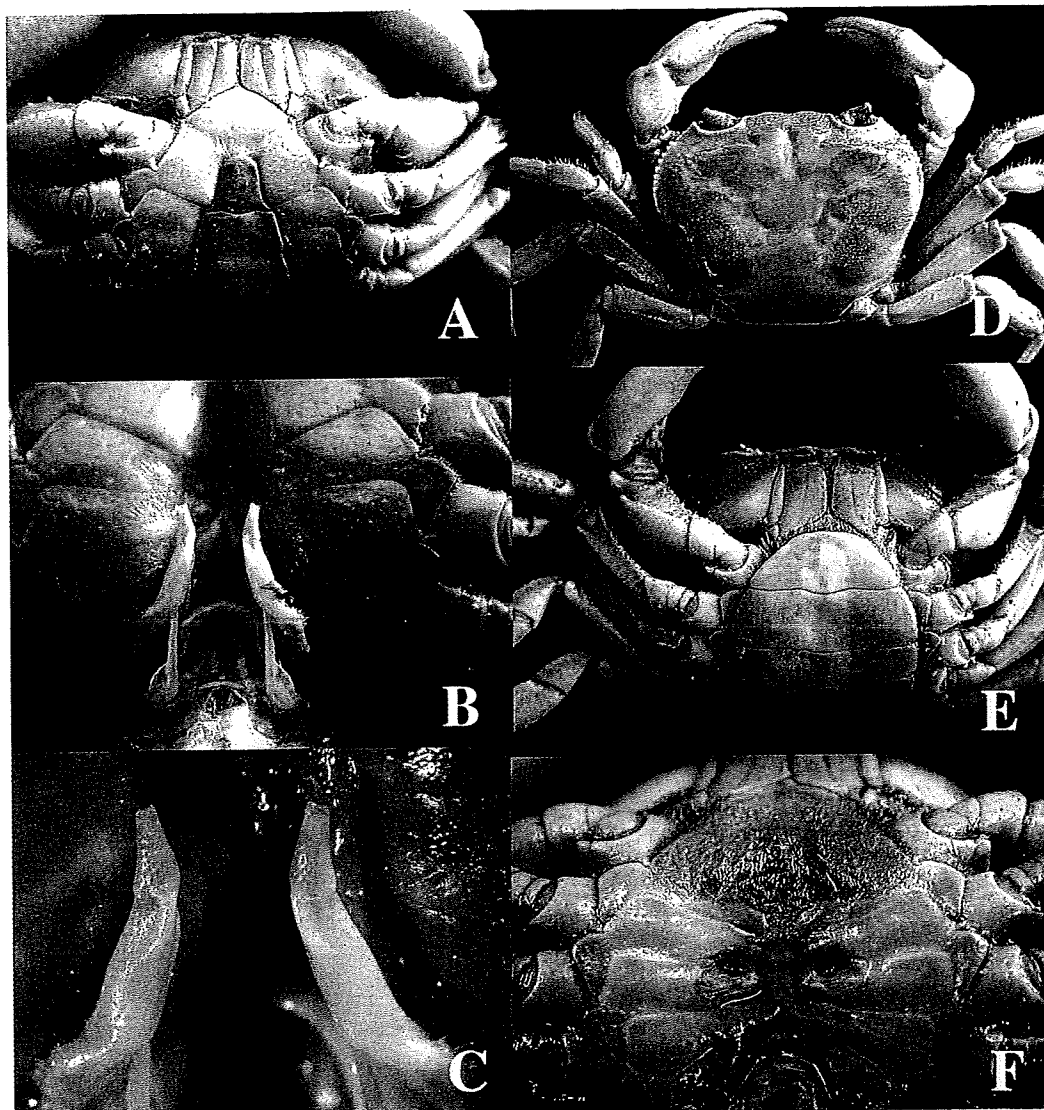
Fig. 3. *Sinopotamon chekiangense* Tai & Song from Yuyao, Zhejiang Province. Male (cb 35.3 mm), abdomen (A) and first pleopod (B, C). Female (cb 29.5 mm), carapace (D), abdomen (E) and genital orifice (F).

convergent posterolateral margins. The male abdomen is becoming narrower distally in this species, but not tapering in *S. chekiangense*, and the terminal segment of the male first pleopod is tapering and weakly directed outward, but not tapering, incised small at its tip, directed outward and dorsad in *S. chekiangense*.

Distribution. Known by Dai *et al*. (1986)[4] and Dai (1999)[1] who mentioned many localities in Hubei Province and some localities in Sichuan Province. According to them, this species lives in the mountain river at the altitude 700-1400 m.

Notes. Metacercariae of *Paragonimus skrjabini* Chen, 1959 were isolated.

Genus *Potamon* Savigny, 1816

Potamon flexum Dai, Song, Li & Liang, 1980

(Figs. 1C, 2C, 5)

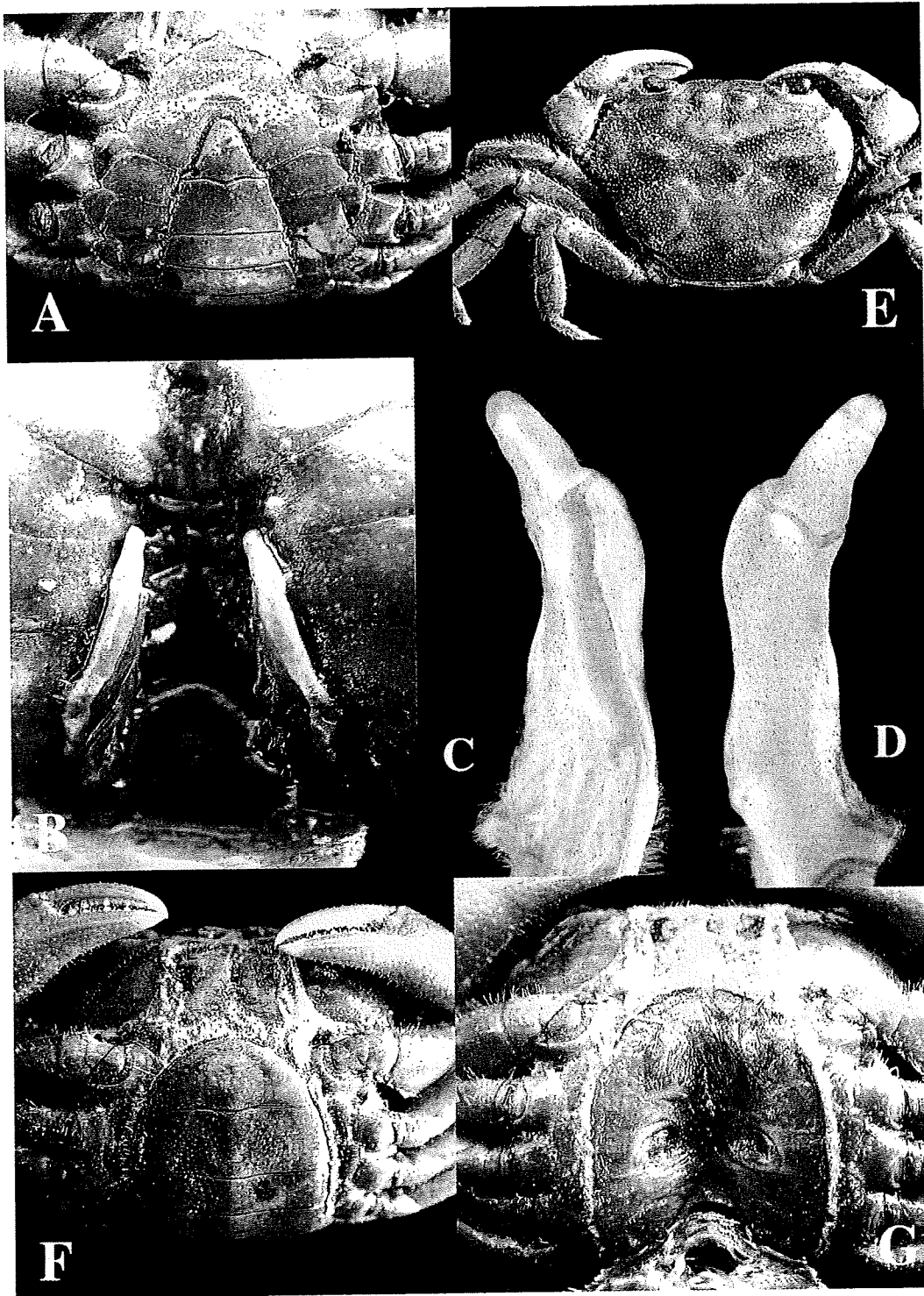*Material examined*. Guoli, Shanjie Village, Beinan Township, Napo County, Baiswe City, Guangxi Zhuang

Fig. 4. *Sinopotamon teritisum* Dai, Chen, Zhang & Lin from Danjiangkou, Hubei Province. Male (cb 31.6 mm), abdomen (A), first pleopod (B-D). Female (cb 25.0 mm), carapace (E), abdomen (F) and genital orifice (G).

Autonomous Region, China（广西壮族自治区百色市那坡百南乡上盖村）— 1♂(cb 56.3 mm, cl 41.3 mm), 1♀(cb 39.5 mm, cl 29.4 mm), May 15, 2007.

Description. Male. Carapace transversely ovate in outline, with convex anterolateral margin rimmed with a narrow edge; dorsal surface rather flattened, roughened with scattered granules of good size mainly on anterior and anterolateral surfaces, uneven, with grooves and depressions symmetrically arranged; frontorbital
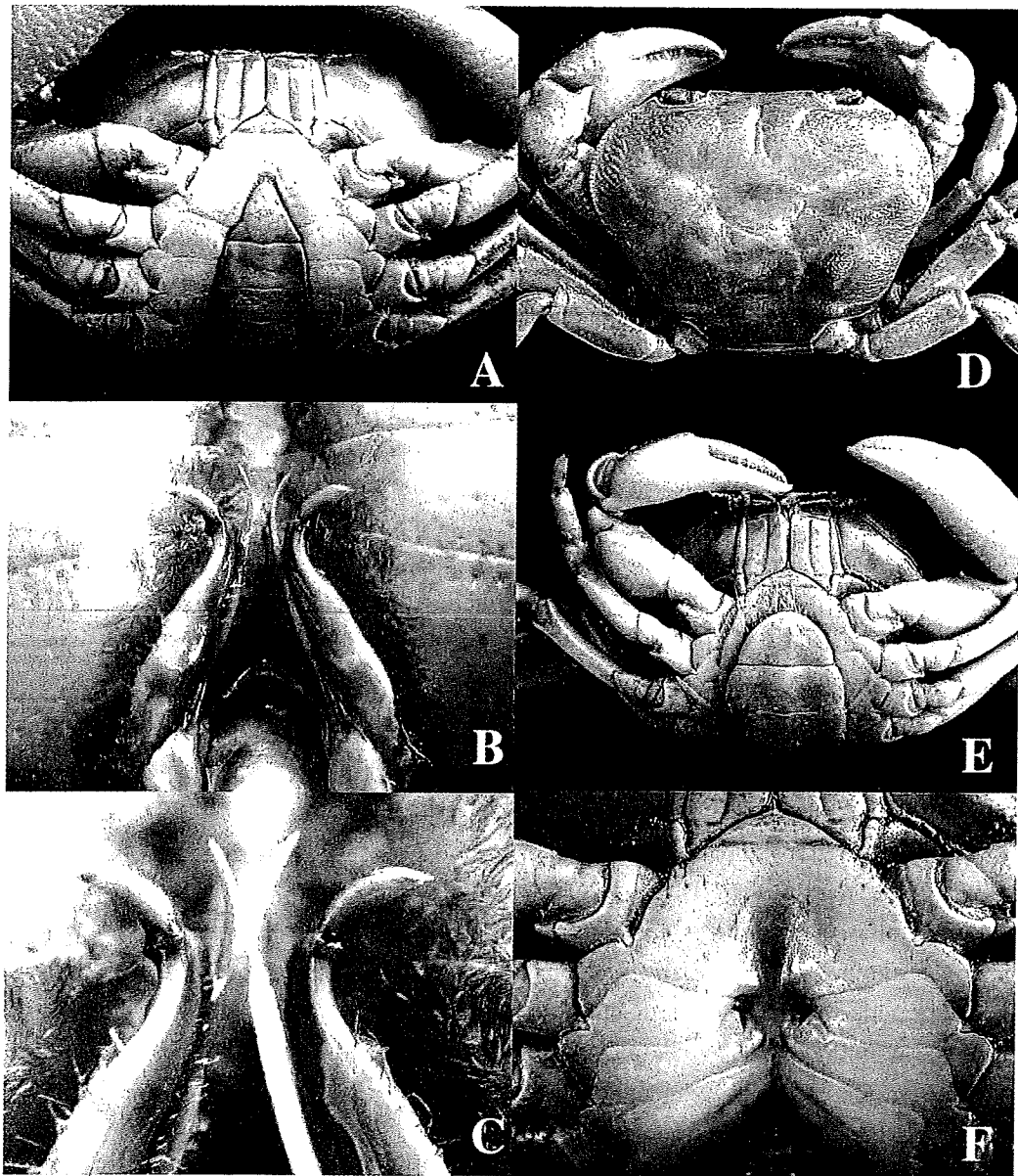
Fig. 5. *Potamon flexum* Dai, Song, Li & Liang from Baiswe, Guangxi Zhuang Autonomous Region. Male (cb 56.3 mm), abdomen (A), first and second pleopods (B, C). Female (cb 39.5 mm), carapace (D), abdomen (E) and genital orifice (F).

margin raised as a narrow ridge, separated from gastric regions by a continuous furrow along margin; some depressions symmetrically arranged around mesogastric region, making an appearance of coarse surface, especially with two prominent furrows running anterolaterally and posterolaterally from lateral angle of mesogastric region. Epibranchial notch small but distinct; anterolateral margin unarmed in front of this notch, anterolateral margin behind this notch strongly arched, fringed with granules which are close together and become smaller posteriorly. Posterolateral margin of carapace strongly convergent, rather concave laterally and dorsally behind rim of anterolateral margin.

Chelipeds heavy, distinctly different in size, roughened with granulated wrinkles; inner angle of carpus armed with a strong upper tubercle and a small lower tubercle. Ambulatory legs stout, smooth, sparsely fringed with short setae; each carpus with a longitudinal depression along anterior margin; each propodus

with a longitudinal median furrow along overall length of upper surface.

Abdomen comparatively narrow; length of sixth segment half of its width; terminal segment as long as wide, triangular, with subacute tip. First pleopod stout; shaft tapering, directed obliquely inward, and then strongly and regularly curved outward together with distal segment; ventral surface of shaft swollen longitudinally; distal segment about one fourth as long as shaft, weakly thickened distally to subterminal part, cut out obliquely at distal part, with sharp tip directed almost transversely. Second pleopod elongated, stalk comparatively thick as well as basal half of terminal segment; distal half of terminal segment semitransparent, tapering, weakly curved outward.

Female. The carapace, chelipeds and ambulatory legs are close to those of the male specimen in hand. Although the granules and depressions on the dorsal surface of the carapace are smaller and shallower than those the male, it is not definite that the differences are due to the smaller size of the specimen or the difference of the sex. The chelipeds are comparatively smaller than those of the male, but there may be no definite sexual differences including the asymmetry of both chelipeds between both specimens of different sexes examined. The abdomen is comparatively narrow, with the prominent sixth and terminal segments; the terminal segment is slightly longer than sixth segment, with subacute distal margin. The genital orifice area occupies the inner one fourth of the sixth sternal segment, narrowing outward; its most part convex dorsally as a dome, with the genital orifice at its innermost part directed inward; the front yard of the genital orifice is sunken and expanded anteriorly.

Remarks. This species was described originally by Dai *et al.* (1980: 369, fig. 1, pl. 1 fig. 1)[5] and additionally by Dai (1999: 183, fig. 97, pl. 11 fig. 8)[1] based on the specimens from the Guangxi Zhuang Autonomous Region, living under stone at about 800 m above sea level. According to these records, this species is among the biggest in the genus *Potamon*, with the maximum size of the carapace breadth being 50 and 46.5 mm in the male and the female, respectively. The male specimen in hand is the biggest known to date.

This species is peculiar in having the uneven dorsal surface of the carapace provided especially with two prominent furrows running anterolaterally and posterolaterally from the lateral angle of the mesogastric region, and also the male first pleopod is much more strongly and regularly curved outward at the distal part of the shaft together with the distal segment than those of the related species.

Distribution. Hitherto known from two localities in the Guangxi Zhuang Autonomous Region. Of 13 species and 4 subspecies of the genus *Potamon* enumerated by Dai (1999)[1] from China, *P. flexum* is only the inhabitant outside the Yunnan Province.

Notes : Metacercariae of *Paragonimus heterotremus* Chen & Hsia, 1964 were isolated.

Literature

1) Dai, A., 1999. *Fauna Sinica. Arthropoda, Crustacea, Malacostraca, Decapoda, Parathelphusidae, Potamidae.* Science Press, xiii + 501 pp., 30 pls. (In Chinese with English abstract)

2) Tai, A.-y. & Y.-c. Sung, 1975. A preliminary study of the freshwater crabs as intermediate hosts of lung flukes from China. *Acta Zool. Sinica*, 21: 169-177, pls. 1-4. (In Chinese with English summary)

3) Dai, A., 1991. Brachyura (freshwater crabs), pp. 387-402. In: *Fauna of Zhejiang, Crustacea*, 481 pp., 4 pls. Zhejiang Science and Technology Publishing House. (In Chinese)

4) Dai, A.-y., G.-x. Chen, S.-q. Zhang & H. Lin, 1986. A study of the freshwater crabs from Hubei Province. *Sinozoologia*, (4): 55-71, pl. 1. (In Chinese with English summary)

5) Dai, A.-y., Y..-z. Song, L.-l. Li & P.-x. Liang, 1980. New species and new record of freshwater crabs from Guangxi. *Acta Zootax. Sinica*, **5**: 369-376. (In Chinese with English summary)

A CD36-related Transmembrane Protein Is Coordinated with an Intracellular Lipid-binding Protein in Selective Carotenoid Transport for Cocoon Coloration*[S]

Takashi Sakudoh[‡], Tetsuya Iizuka[§], Junko Narukawa[¶], Hideki Sezutsu[§], Isao Kobayashi[§], Seigo Kuwazaki[¶], Yutaka Banno[∥], Akitoshi Kitamura[**], Hiromu Sugiyama[‡‡], Naoko Takada[‡], Hirofumi Fujimoto[‡], Keiko Kadono-Okuda[¶], Kazuei Mita[¶], Toshiki Tamura[§], Kimiko Yamamoto[¶], and Kozo Tsuchida[‡1]

From the [‡]Division of Radiological Protection and Biology, National Institute of Infectious Diseases, Shinjuku, Tokyo 162-8640, the [§]Transgenic Silkworm Research Center and [¶]Insect Genome Research Unit, National Institute of Agrobiological Sciences, Tsukuba, Ibaraki 305-8634, the [∥]Genetic Resources Technology, Kyushu University, Fukuoka, Fukuoka 812-8581, the [**]Life Science Division, Fuji Chemical Industry Co., Ltd., Nakaniikawa, Toyama 930-0397, and the [‡‡]Department of Parasitology, National Institute of Infectious Diseases, Shinjuku, Tokyo 162-8640, Japan

The transport pathway of specific dietary carotenoids from the midgut lumen to the silk gland in the silkworm, *Bombyx mori*, is a model system for selective carotenoid transport because several genetic mutants with defects in parts of this pathway have been identified that manifest altered cocoon pigmentation. In the wild-type silkworm, which has both genes, *Yellow blood* (*Y*) and *Yellow cocoon* (*C*), lutein is transferred selectively from the hemolymph lipoprotein to the silk gland cells where it is accumulated into the cocoon. The *Y* gene encodes an intracellular carotenoid-binding protein (CBP) containing a lipid-binding domain known as the steroidogenic acute regulatory protein-related lipid transfer domain. Positional cloning and transgenic rescue experiments revealed that the *C* gene encodes *Cameo2*, a transmembrane protein gene belonging to the CD36 family genes, some of which, such as the mammalian *SR-BI* and the fruit fly *ninaD*, are reported as lipoprotein receptors or implicated in carotenoid transport for visual system. In *C* mutant larvae, Cameo2 expression was strongly repressed in the silk gland in a specific manner, resulting in colorless silk glands and white cocoons. The developmental profile of *Cameo2* expression, *CBP* expression, and lutein pigmentation in the silk gland of the yellow cocoon strain were correlated. We hypothesize that selective delivery of lutein to specific tissue requires the combination of two components: 1) CBP as a carotenoid transporter in cytosol and 2) Cameo2 as a transmembrane receptor on the surface of the cells.

All organisms exposed to light contain carotenoids, which are yellow to red C_{40} hydrophobic isoprenoid pigments. Carotenoids play pivotal roles in living organisms as precursors of vitamin A, antioxidants, and colorants (1). Their potential roles in medicine have recently been investigated. For example, macular accumulation of the carotenoids lutein and zeaxanthin is associated with a decreased risk of age-related macular degeneration (2), the leading cause of blindness in the developed world. Although plants, certain fungi, and bacteria synthesize carotenoids, animals appear to be incapable of synthesizing these molecules *de novo*. Therefore, animals must acquire carotenoids from dietary sources, and subsequently transport them to cells of target tissues.

The delivery of lipids, including carotenoids, to cells can be divided into three categories: 1) enzyme-mediated processes, such as the action of lipoprotein lipase on very low density lipoproteins, which converts a lipoprotein-bound lipid, triacylglycerol, into a water-soluble product, fatty acid, which diffuses into cells and leaves behind in the blood a lipoprotein product depleted in triacylglycerol (3); 2) receptor-mediated endocytosis, such as the uptake of low density lipoproteins by low density lipoprotein receptor, in which the entire lipoprotein particle is taken into the cell and metabolized (4); and 3) the delivery of specific lipids to specific tissues devoid of lipoprotein degradation, called selective lipid transport, such as the delivery of cholesterol ester from high density lipoprotein (HDL)[2] to the adrenal gland (5). The first two mechanisms have been extensively studied in vertebrates. However, the third mechanism, which clearly occurs in both vertebrates and invertebrates, is poorly understood.

In the domesticated silkworm, *Bombyx mori*, previous works have demonstrated the existence of tissue-specific delivery of

[2] The abbreviations used are: HDL, high density lipoprotein; *C*, *Yellow cocoon*; Cameo, *C* locus-associated membrane protein homologous to a mammalian HDL receptor; CBP, carotenoid-binding protein; SR-BI, scavenger receptor class B type I; RT, reverse transcriptase; SNP, single nucleotide polymorphism; START, steroidogenic acute regulatory protein-related lipid transfer; UAS, upstream activating sequence; IV0, day 0 of the fourth instar; V0, day 0 of the fifth instar; W0, day 0 of the wandering stage; *Y*, *Yellow blood*; HPLC, high-performance liquid chromatography; EGFP, enhanced green fluorescent protein.

- 558 -
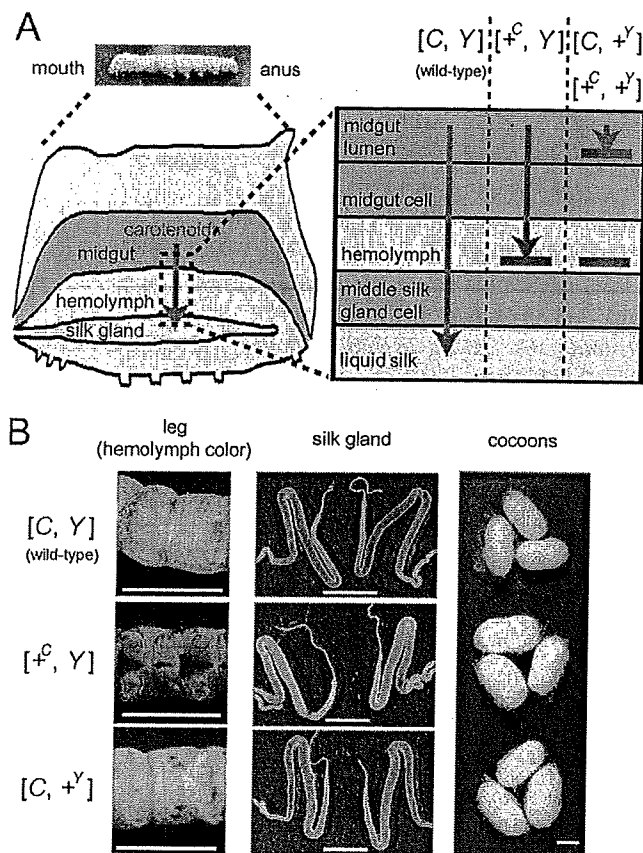
Cameo2 Is Coordinated with CBP in Carotenoid Transport

FIGURE 1. **Transport of lutein by the Yellow cocoon (C) gene and the Yellow blood (Y) gene.** *A,* schematic representation of the functions of the *C* and *Y* genes in the carotenoid transport system of the silkworm. $+^C$ and $+^Y$ represent a recessive allele of the *C* and *Y* genes, respectively. *B,* color phenotype of the hemolymph, silk gland, and cocoons. The hemolymph color is visible on the abdominal legs where the skin is relatively transparent. The silk glands are paired organs. The c10, c05, and FL501 $(+^Y)$ strains were used as the genotypes of $[C, Y]$, $[+^C, Y]$, and $[C, +^Y]$, respectively. The silkworm with the genotype of $[+^C, +^Y]$ exhibits colorless hemolymph and produces white cocoons, similar to $[C, +^Y]$. Legs were at day 3 of the fifth larval instar (V3). Silk glands were at day 0 of the wandering stage (W0). The lutein content of the middle silk gland of $[C, Y]$ was about 30-fold higher than that of $[+^C, Y]$ (data not shown). The *black* color of the larval skin of the c05 strain was due to the larval marker gene, p^s. *Scale bar,* 1 cm.

specific carotenoids (6–9). The wild-type silkworm feeds on carotenoid-rich mulberry leaves in the larval stage. Carotenoids are then absorbed into the midgut epithelium, transferred to the hemolymph lipoprotein, lipophorin, and accumulated in the middle silk gland, resulting in yellow hemolymph and the formation of a yellow cocoon (Fig. 1, *A* and *B*). Lipophorin facilitates lipid transport in insects in a selective manner (10). Over the 4000 year history of sericulture, several mutants have been noted that produce white cocoons due to defect in carotenoid transport (11). Among these are mutants in the selective transport of carotenoids from lipophorin to the middle silk gland. Molecular cloning of the genes responsible for these mutants therefore provides tools to determine the molecular mechanism of selective carotenoid transport.

The *Yellow blood (Y)* gene on chromosome 2 of *B. mori* controls transport of carotenoids from the midgut lumen to the midgut epithelium and from the lipophorin to the middle silk gland cells (Fig. 1A) (7–9). We have reported previously that the

Y gene encodes an intracellular carotenoid-binding protein (CBP) (12), which was identified based on a combination of expression analysis (12, 13), restriction fragment length mapping (14), genomic sequence analysis (15, 16), and transgenic rescue of phenotype (16). CBP is a 33-kDa protein containing a lipid-binding domain known as the steroidogenic acute regulatory protein-related lipid transfer (START) domain (17). CBP is expressed in the midgut, the middle silk gland, testis, and ovary in the dominant *Y* allele strain ("*X* allele strain" represents the strain harboring the homozygous *X* allele), producing yellow cocoons. In *Y* mutants homozygous for the recessive $+^Y$ allele, genomic deletion of the *CBP* gene leads to complete absence of the CBP protein. The midgut epithelium, therefore, poorly absorbs carotenoids, resulting in colorless hemolymph, colorless middle silk gland, and white cocoons (Fig. 1B).

The *Yellow cocoon (C)* gene on chromosome 12 controls transport of carotenoids, mainly lutein, from lipophorin to the middle silk gland cells (Fig. 1A) (11, 18). The middle silk glands of the *C* mutants, homozygous for the recessive $+^C$ allele, have a defect in the cellular uptake of lutein and are, therefore, colorless even in the presence of yellow hemolymph mediated by the dominant *Y* allele of the *Y* gene, resulting in white cocoons (Fig. 1B). Selective transport of lutein from lipophorin to middle silk gland cells by the dominant *C* allele requires the *Y* allele (19, 20). Thus, molecular cloning of the *C* gene was expected to offer a novel molecular component that facilitates selective transport of lutein in coordination with CBP in middle silk gland cells.

In the present study, the *C* gene was cloned using a positional cloning method, resulting in identification of Cameo2 (*C* locus associated membrane protein homologous to a mammalian HDL receptor-2). Cameo2 belongs to the CD36 family, including scavenger receptor class B type I (SR-BI), a transmembrane receptor of mammalian HDL (5). A molecular pathway for selective lutein transport in the body of the silkworm by a combination of Cameo2 and CBP is proposed.

EXPERIMENTAL PROCEDURES

Silkworm Strains—The c04, c05, c10, c11, c43 (*Pk*), e09, FL501 (*Y/+^Y*), and FL501 (*+^Y/+^Y*) strains have been preserved at the silkworm stock center of Kyushu University, Fukuoka, Japan. The number 925 and w1-pnd strains have been preserved in the National Institute of Agrobiological Sciences, Ibaraki, Japan. The N4 strain has been preserved at the National Institute of Infectious Diseases, Tokyo, Japan. The Kinshu X Showa F1 hybrids were a generous gift from Dr. Toru Shimada (University of Tokyo, Tokyo, Japan). The larvae were reared on mulberry leaves or an artificial diet made from mulberry leaves (Nihon Nosan Kogyo Co., Yokohama, Japan). Data regarding the origin, genotype, and phenotype of these strains are summarized in supplemental Table S1. The first days corresponding to the developmental stages of the third to fourth larval ecdysis, the fourth to fifth larval ecdysis, and wandering, a characteristic behavior with enhanced locomotory activity just before spinning cocoons, were designated as IV0, V0, and W0, respectively.

Crossing and Genomic Extraction for Mapping of the C Gene—Two silkworm strains, c11 (*C/C, Y/Y*, yellow cocoon with yel-

- 559 -

low hemolymph) and number 925 ($+^C/+^C$, *Y/Y*, white cocoon with yellow hemolymph) were used. Single-pair crosses between number 925 and c11 produced F1 offspring. As female recombination is uncommon in *B. mori* (21), BF1 progeny from the single-pair cross between female number 925 and males of F1 (number 925 X c11) were used for recombination mapping. The number of single-pair matings for BF1 progeny was 18. Each of the total of 1775 BF1 individuals was named, phenotypically recorded, and subjected to genomic DNA extraction using DNAzol Reagent (Invitrogen). None of the BF1 individuals analyzed showed colorless hemolymph.

Mapping Using Single Nucleotide Polymorphism (SNP) Markers—For mapping using the BF1 progeny, PCR primer sets were generated at each position on chromosome 12, and primer sets with that the PCR products showed polymorphism between parents were used for SNP markers. The PCR primers used for SNP analysis are listed in supplemental Table S2. The PCR products treated with ExoSAP-It (U. S. Biochemical Corp.) were subjected to direct sequencing.

RNA Extraction—Total RNA was isolated from tissues washed in insect saline (20 mM sodium phosphate buffer, 150 mM sodium chloride, pH 6.7) with TRIzol reagent (Invitrogen). Before addition to TRIzol reagent, the silk gland and midgut were frozen in liquid nitrogen and broken into fine pieces. The other tissues were syringe-homogenized in TRIzol reagent.

Comparison of the Cameo1 and Cameo2 cDNA Sequences between the C and $+^C$ Allele Strains—*Cameo1* and *Cameo2* were amplified from the middle silk gland of each strain via reverse transcription (RT)-PCR and directly sequenced. The PCR primers used for each gene and strain are listed in supplemental Table S3.

Data Base Search for Cameo1 and Cameo2 Homologs in the Silkworm—The silkworm genome contained 13 annotated genes homologous to *Cameo1* and *Cameo2*, which were retrieved from the KAIKObase system through a keyword search using "CD36" as the query. The TBLASTN program was used to search for all genes homologous to *Cameo1* and *Cameo2* in the silkworm genome sequence (22) and EST data base (23) with a cutoff *E* value of 5×10^{-3} and the results did not include any others besides these 13 genes. One of these homologous genes, *SNMP1*, has been cloned (24), and recently 10 of them were reported and named by independent data base searches (25, 26). We use in this paper the same names for the total 11 genes and term the other two genes, BGIBMGA13436 and BGIBMGA13438 in the China gene model ("BGIBMGA" is a prefix for gene name), SCRB14 and SCRB15, respectively.

Phylogenetic Analysis of the Protein Sequences Homologous to Cameo1 and Cameo2—Alignment of the hypothetical protein sequences was performed using Clustal W2 (27). A phylogenetic tree was then constructed with the neighbor-joining method using Clustal X2 (27).

Northern Blotting—For *Cameo2*, a ^{32}P-labeled riboprobe was synthesized from the N-0394 EST clone. The insert of N-0394 contained the 3' part (1016 bp) of the open reading frame and the 5' part (1209 bp) of the 3'-untranslated region of *Cameo2*. No silkworm repetitive sequence was found in the insert. Total RNA was electrophoresed on 1% agarose gels containing formaldehyde and transferred onto Hybond N$^+$ membrane (GE

Healthcare UK). Hybridization was performed with Ultrahyb (Ambion, Austin, TX).

RT-PCR Analysis of Tissue Distribution of Cameo1, Cameo2, and rpL3—Primer1-1 (5'-CTGAAAGTGGAGCAGTTGGG-TCCTTACG-3') and Primer1-4 (5'-CGGACACCTTGACGA-CCCTGGGCTGGTG-3') for *Cameo1*, Primer2-3 (5'-GGAC-CAGGTCACCGGCATGAACCCGGATC-3') and Primer2-2 (5'-CGTCCTCAGCTCCGAAATGATTTTTGGATC-3') for *Cameo2*, and Primer-rpL3-real-cDNA1 (5'-TTCCCGAAAG-ACGACCCTAG-3') and Primer-rpL3-real-cDNA2 (5'-CTC-AATGTATCCAACAACACCGAC-3') for *rpL3* were used.

Analysis of Carotenoid Composition of the Middle Silk Gland—Samples of the middle silk gland cut into small pieces less than 1 mm length (~200 mg) were transferred into a glass centrifuge tube with 5 ml of distilled water and 2 g of glass beads (1 mm diameter) as agitating aid were added. After heating at 90 °C for 15 min, eluate was collected. 5 ml of 80% ethanol with butylhydroxytoluene as an antioxidizing agent at a concentration of 10 µg/ml was added to the residue, followed by heating at 90 °C for 10 min with vortexing at intervals. The eluate was then collected. Extraction with 80% ethanol was repeated three times. 3 ml of 100% ethanol with butylhydroxytoluene was added to the residue, followed by heating at 90 °C for 10 min with vortexing at intervals. The eluate was then collected. Extraction with ethanol was repeated until the residue became colorless. All of the collected extracts were pooled, and ethanol was evaporated. 1 g of sodium sulfate decahydrate was then added followed by extraction three times with 5 ml of petroleum ether. 9 ml of acetone was added to the aqueous layer, then extracted with 5 ml of petroleum ether three times. The organic phase was dried over anhydrous sodium sulfate and evaporated. The residue was resolved in acetone and used for carotenoid analysis by high performance liquid chromatography (HPLC). A reverse-phase column (YMC carotenoid 5 µm (4.6 X 250 mm); Waters Co., Milford, MA) was used under the following conditions: temperature, 25 °C; flow rate, 1 ml/min; mobile phase, A, methanol; B, *t*-butylmethylether; C, 1% (v/v) aqueous phosphoric acid; a 15-min linear gradient from 81% A, 15% B, 4% C to 66% A, 30% B, 4% C; an 8-min linear gradient to 16% A, 80% B, 4% C, a 4-min hold at 16% A, 80% B, 4% C, then back to 81% A, 15% B, 4% C, and an 8-min hold at 81% A, 15% B, 4% C.

Quantification of Transcripts by Real Time PCR—Single-stranded cDNAs from various tissue samples were synthesized from total RNAs with Superscript III reverse transcriptase (Invitrogen) with oligo(dT) primer, and treated with RNase H (Takara, Kyoto, Japan). Quantification of transcripts was carried out by real time PCR using these cDNAs as templates with LightCycler FastStartDNA MasterPLUS SYBR Green I (Roche) and LightCycler DX400 (Roche). The primer pairs used for detection of *Cameo1*, *Cameo2*, *CBP*, and *rpL3* were Primer1-1 and Primer1-6 (5'-CGCCACAGTCGCTATTATAGGGTTG-ATGC-3'); Primer2-19 (5'-AGTGTTAGAGGAGGTGCACC-AGCTC-3') and Primer2-16 (5'-CAGTCCGTTTTGAACCC-CACTCTCC-3'); PrimerCBP-1 (5'-ATGGCCGACTCTACG-TCGAAAAGCG-3') and PrimerCBP-18 (5'-GCCTTCA-ACTTTCCTTGACTCCACGACG-3'); and Primer-rpL3-real-cDNA1 and Primer-rpL3-real-cDNA2, respectively. For *Cameo1*, *Cameo2*, and *rpL3*, absence of mutation in the anneal-

– 560 –

ing sites of these primers among the analyzed strains was confirmed (supplemental Fig. S2). Serial dilutions of plasmids containing the cDNA sequences were used as standards. Transcript levels of *Cameo1*, *Cameo2*, and *CBP* were normalized with the level of the *rpL3* transcript in the same samples, as described previously (28).

Analysis of F1 SNPs of Cameo1 and Cameo2—The cDNA sequences of *Cameo1* and *Cameo2* of each parental strain were aligned (supplemental Fig. S2). Then primer pairs, Primer1-3 (5′-GAGGGCGTTCGGTACGCGGCCAACGACTC-3′) and Primer1-2 (5′-CTGGATCTTGCTGGGGTAGTACGGGTC-3′) for *Cameo1*, Primer1-25 (5′-TATCAACAACGTGTTGC-CGGACC-3′) and Primer1-16 (5′-GTGAGGGTGTAGAGC-GCGTATG-3′) for *Cameo1*, Primer2-19 and Primer2-16 for *Cameo2*, and Primer2-21 (5′-TCCTTACCGTTACCAGGAG-CATAG-3′) and Primer2-20 (5′-GCGGTTATAACGTCAAT-GGTTGTG-3′) for *Cameo2* were designed according to the conserved nucleotide sequence for PCR amplification of the cDNA and genomic DNA of the parental and F1 strains, and the PCR products by these primer pairs were directly sequenced with Primer1-2, Primer1-25, Primer2-18 (5′-TTG-GAGCATTCGCCGTCG-3′), and Primer2-21, respectively.

Western Blotting—A rabbit polyclonal antibody against Cameo2 was raised against the synthetic peptide (C-)NGLKY-NKYEVNERS (amino acids 295–308, corresponding to the putative extracellular domain (Fig. 3*B*)) coupled to keyhole limpet hemocyanin and affinity purified by Operon Biotechnologies (Tokyo, Japan). For Western blotting analysis of the membrane fraction, 100 pieces of the silk gland of each strain on the day 0 of the wandering stage (W0) was homogenized in ice-cold insect saline containing a protease inhibitor mixture (Protease Inhibitor Mixture Set III, EDTA-free, Calbiochem, San Diego, CA) using a Polytron homogenizer. The homogenate was centrifuged at 800 × *g* for 10 min, and the supernatant was filtered through cheesecloth and centrifuged at 1,000 × *g* for 10 min. The membranes were then pelleted by centrifugation at 100,000 × *g* for 1 h and resuspended in 20 mM Tris-HCl, 150 mM NaCl, 2 mM CaCl$_2$, 0.1 mM phenylmethylsulfonyl fluoride, pH 7.4, at a concentration of 10 mg of protein/ml. Then, the same volume of 80 mM *n*-octylglucoside was added for solubilization. After mixing for 1 h, insoluble material was removed by centrifugation at 100,000 × *g* for 1 h. The concentration of *n*-octylglucoside in soluble extract was adjusted to 5 mM by addition of 7 volumes of 20 mM Tris-HCl buffer, and centrifuged at 100,000 × *g*, 1 h to collect precipitate. The pellet was resuspended again in 20 mM Tris-HCl, 150 mM NaCl. The protein concentration was determined with the Bradford method (Protein Assay solution; Bio-Rad). Then, 25 μg of protein was separated by SDS-PAGE, transferred to polyvinylidene difluoride membrane, and probed with the anti-Cameo2 antibody and a sheep anti-rabbit IgG-conjugated alkaline phosphatase (Jackson ImmunoResearch Laboratory, West Grove, PA). The signals were detected by AP-conjugate Substrate Kit (Bio-Rad).

Immunohistchemistry—Cross-sections of the middle silk gland from the region of "MSG-3" in Fig. 5*C* were deparaffinized in xylene, rehydrated through graded ethanol solutions, and quenched with a 30-min immersion in 0.3% hydrogen peroxide in methanol. Sections were blocked for 30 min in normal goat serum in phosphate-buffered saline, and incubated with the Cameo2 antibody (at 1:1000 dilution) used for the Western blotting experiment overnight at 4 °C. Sections were rinsed in phosphate-buffered saline, and incubated for 30 min with a biotinylated goat anti-rabbit IgG (at 1:200 dilution). The slides were developed using the ABC Vectastain Elite kit (Vector Labs, Burlingame, CA) following the manufacturer's instructions. The slides were counterstained in Mayer hematoxylin.

Silkworm Transgenesis—We first attempted to produce the nondiapausing strain with the phenotype of yellow hemolymph and white cocoons. The number 925 strain of the genotype [*Y*, +^{C}] was crossed with the w1-pnd strain, a nondiapausing strain with the genotype [+^{Y}, +^{C}] used for transgenesis of *B. mori* (29). By sib mating of the progeny, a nondiapausing strain with the phenotype of yellow hemolymph and white cocoons, termed w1-pnd-925, was established.

For transgenic expression of Cameo2 in the w1-pnd-925 strain by the binary GAL4/upstream activating sequence (*UAS*) system (30), *Cameo2* was amplified by RT-PCR from the middle silk gland of the N4 strain with Primer2-13 (5′-ATGCTCTAG-ATTCCTTGTGATAATCGCGGC-3′) and Primer2-10 (5′-ATGCTCTAGACATACGGACTCATTCCAATG-3′), both of which have an XbaI site. The PCR product was subcloned into the pGEM T-vector, and the subcloned product was digested with XbaI. The fragment was ligated into the vector *pBacMCS-[UAS-3xP3-EGFP]* (16) previously digested with BlnI. The resulting effector construct *pBacMCS[UAS-Cameo2-3xP3-EGFP]* was confirmed by DNA sequencing. For the effector strains, the effector construct and the helper plasmid, pHA3PIG (29), were injected into preblastoderm embryos of the w1-pnd-925 strain at a concentration of 0.2 mg/ml. After sib selection based on the presence of EGFP fluorescence in the eye by the *3xP3-EGFP* gene, G1 male moths of a UAS-Cameo2 (UAS) line with the phenotype of yellow hemolymph and white cocoons were crossed with females of the Ser1-GAL4 (GAL4) line with the phenotype of colorless hemolymph and white cocoons, which drives target gene expression in the middle silk gland and has a marker fluorescence in the eye by the *3xP3-DsRed* gene (31). Because the transgene was supposed to be homozygous in the GAL4 line, the progeny of the cross between the UAS line and GAL4 line showed two different marker phenotypes of eye color: both DsRed- and EGFP-positive, GAL4/UAS line (Ser1-GAL4(+), UAS-Cameo2(+)); and only DsRed-positive, GAL4 line (Ser1-GAL4(+), UAS-Cameo2(−)). Data from the individuals exhibiting colorless hemolymph in the larval stage, which had colorless silk glands and produced white cocoons, were not presented in Fig. 7, *B–E*. Experimental procedures for determination of the *Cameo1* and *Cameo2* cDNA sequence and Southern blotting are described under supplemental data.

RESULTS

Mapping of the C Locus—To identify a candidate physical region for the *C* locus, we performed genetic linkage analysis using SNP markers (32, 33). First, the *C* locus was roughly mapped with 75 BF1 individuals, and the *C*-linked region was narrowed to the 1.94 Mb range on chromosome 12 between two SNP markers, 12-055 and 12-056 (Fig. 2*A*). Then, novel

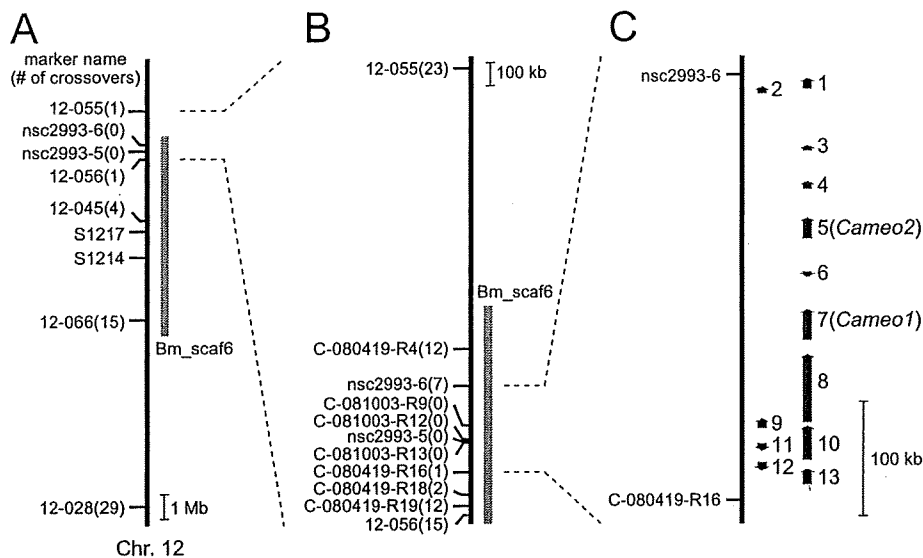*Cameo2 Is Coordinated with CBP in Carotenoid Transport*

FIGURE 2. **Mapping of the C gene on the chromosome 12.** *A,* rough mapping with 75 individuals. *Small horizontal lines* on the *vertical bars* of chromosome 12 denote the positions of crossover events with the name of the SNP maker and the number of recombinants. Recently, Li and colleagues (63) independently showed that the *C* locus was closer to SSR marker S1217 than S1214, consistent with our results. *B,* finer mapping with 1700 individuals. *C,* physical map of chromosome 12 near the *C* locus with the predicted gene. *Vertical arrows* indicate the orientation and relative size of the 13 putative genes predicted by the China gene model (22). *1,* BGIBMGA010481 (SMAD homolog); *2,* BGIBMGA010480 (unknown); *3,* BGIBMGA010479 (unknown); *4,* BGIBMGA010478 (similar to the CG7231 gene of *D. melanogaster,* whose molecular function is unknown); *5,* BGIBMGA010477 (*Cameo2*); *6,* BGIBMGA010502 (unknown); *7,* BGIBMGA010476 (*Cameo1*); *8,* BGIBMGA010475 (dynein heavy chain homolog); *9,* BGIBMGA010474 (dynein heavy chain homolog); *10,* BGIBMGA010473 (dynein heavy chain homolog); *11,* BGIBMGA010503 (homolog of SprT-like metalloproteases with zinc finger domain); *12,* BGIBMGA010504 (tetraspanin homolog); *13,* BGIBMGA010472 (similar to muscle-specific protein 300, involved in cytoskeleton organization).

primer sets were designed in the narrowed range, and finer mapping was performed with 1700 BF1 individuals. As a result, the *C*-linked region was further narrowed to the 375-kb range between two SNP markers, nsc2993-6 and C-080419-R16, which was on one scaffold, Bm_scaf6 (Fig. 2*B*).

Candidates for the C Gene—Thirteen genes were predicted within the narrowed region by the China gene model at KAIKObase (22) (Fig. 2*C*). Among them, two genes were found to encode proteins homologous to SR-BI, a mammalian transmembrane cell surface receptor for HDL (5, 34–36). SR-BI mediates cellular uptake of cholesteryl ester from HDL in a selective manner. SR-BI was proposed to form a hydrophobic channel along which cholesteryl esters migrate (37). Furthermore, mutants of the *ninaD* gene, a homolog of SR-BI in the fruit fly *Drosophila melanogaster,* was reported to affect carotenoid uptake in gut for visual chromophore synthesis (38–40), and SR-BI was also implicated in cellular carotenoid absorption (41–44). Therefore, we considered these two genes to be strong candidates for the *C* gene, and designated the gene nearer the SNP marker C-080419-R16 *Cameo1* and the other *Cameo2.*

Characterization of the Cameo1 and Cameo2 Sequences—We determined each cDNA sequence containing the full-length of the open reading frame of *Cameo1* and *Cameo2* from a *C* allele strain. *Cameo1* and *Cameo2* span a region of 120 kb in the Bm_scaf6, and are composed of 11 and 10 exons, respectively (Fig. 3*A*). The deduced amino acid sequence indicated that Cameo1 and Cameo2 are a 56.2-kDa protein of 495 amino acids and a 56.0-kDa protein of 494 amino acids, respectively

(Fig. 3*B*). The degree of identity between Cameo1 and Cameo2 is 28%. Cameo1 and Cameo2 share 32 and 26% amino acid identity, respectively, with the human SR-BI and 32 and 31% identity, respectively, with the fruit fly NinaD. TMHMM version 2.0 (45), software for prediction of transmembrane helices, predicted that both gene products are comprised of a large extracellular loop, anchored to the plasma membrane on each side by transmembrane domains adjacent to short cytoplasmic N-terminal and C-terminal domains (Fig. 3*B*). SignalP 3.0-HMM (46), a program for prediction of signal peptide, predicted that the N termini of Cameo1 and Cameo2 are signal peptides with a probability of 29 and 95%, respectively. The cleavage site with maximum probability was near the C terminus of the N-terminal putative transmembrane domain in Cameo1 and Cameo2, respectively (Fig. 3*B, arrow*). Therefore, we tentatively propose that Cameo1 and Cameo2 are single- or double-pass transmembrane proteins (Fig. 3*C*).

It could be noted that the existence of the N-terminal transmembrane helix in SR-BI homologs, CD36 family genes, has been a matter of debate (5, 47), and some of them were similarly predicted to have a single- or double-pass transmembrane structure at various ratios (Fig. 3*C*).

There are 13 other genes homologous to *Cameo1* and *Cameo2* in the silkworm genome data base (22). These genes were distributed or tandemly positioned in several chromosomes (Fig. 3*D*). No homologous genes other than *Cameo1* and *Cameo2* were found on chromosome 12, where the *C* locus lies. The phylogenetic tree of these silkworm genes was generated with the CD36 family genes from insects and mammals (Fig. 3*E*). As indicated in a previous study in Dipterans (48), the insect genes could be largely divided into three groups, and *Cameo1* and *Cameo2* fall into the Group 2. Group 2 contains functionally characterized genes of *D. melanogaster. Santa maria* is implicated in cellular uptake of carotenoids in extraretinal neural cells in heads (40), *crq* is required for efficient phagocytosis of apoptotic cells (49), and *pes* was identified as a host factor required for the uptake of mycobacteria (50). The orthologous relationships of the Group 2 genes were not clear. SNMP in Group 3 is required for chemoreception of (*Z*)-11-octadecenyl acetate in olfactory neurons of *D. melanogaster* (24, 51, 52). The mammalian homologs formed a distinct group. CD36 is implicated in cellular uptake of long-chain fatty acids (53).

Comparison of the Nucleotide Sequences of Cameo1 and Cameo2 between the C and +^C Allele Strains—Southern blotting analysis suggested that the silkworm has a single copy of

– 562 –

Cameo2 Is Coordinated with CBP in Carotenoid Transport

the *Cameo1* and *Cameo2* genes irrespective of the genotype of the *C* gene (supplemental Fig. S1). Then, to examine the relationship between the *C* gene with *Cameo1* and *Cameo2*, we compared the mRNA sequences of *Cameo1* and *Cameo2*

among three *C* allele strains and four $+^C$ allele strains (supplemental Fig. S2). The mRNA sequences of *Cameo1* and *Cameo2* were well conserved and absent of indels and premature stop codons, whereas one nonsynonymous mutation in Cameo1

A

B

C

	double-pass	single-pass
Cameo1	70 %	29 %
Cameo2	5 %	95 %
SR-BI (human)	32 %	68 %
SR-BI (mouse)	35 %	65 %
CD36 (human)	93 %	7 %
NinaD	84 %	15 %
Santa maria	97 %	3 %

D

E

– 563 –